2013 IREP Symposium-Bulk Power System Dynamics and Control –IX (IREP), August 25-30, 2013, Rethymnon, Greece

Dynamic Load Dispatch for Power System Robust Security Against Uncertainties

Naoto Yorino, Yutaka Sasaki, Emil Popov Hristov, Yoshifumi Zoka
Hiroshima University

Yoshiharu Okumoto
Chugoku Industrial Innovation Center

Abstract

The rapid growth in the electricity demand and expansion of renewable energy (RE) generation are presenting serious challenges for the optimal network operation. The future perspective of the dramatic increase in renewable generation, such as wind and solar energy will lead to severe problems related to the load dispatch. Power system security is threatened due to increase in the uncertainties of RE outputs and the reduction of controllable resources.

This paper investigates power system "robust security" in relation with the increase in the uncertainties and the decrease in system control ability. A new concept of robust security and its security regions is defined and then a new technique for real-time dynamic ELD is proposed. It is guaranteed secure operation in the security region and mitigating the irregularity associated with renewable power generation. Key issue is an effective treatment of uncertainties caused by RE forecast and an efficient solution for real-time management over the limited control resources of a power system. The flexible operational outcome of the proposed approach satisfies the economical requirements and reliability against uncertainties. The proposed method is also useful to investigate the limitation of RE under given ability of real-time generation control. Critical problems anticipated in the future are further investigated from the point of view of robust security concerned with the load dispatch. Robust security for West Japan system is also investigated from the present up to 2030 concerned with the transient stability.

Introduction

The use of renewable energy is expected to grow substantially in the near future. A reasonable estimation is that 20-30% of the energy will be delivered through such sources in the upcoming 15 years in considerable number of power systems. Photovoltaic (PV) as well as wind turbine (WT) systems are amongst such predictions, but are prone to cause degradation of power quality as well as grid security due to unforeseen weather conditions. Continuous intermittency incurs into sudden changes in the output, leading to uncertainty such as significant ramp effect. The influence of the increasing usage of renewable energy technology requires essentially new methodologies for power system operation.

In various power systems, unpredictable uncertainties have increased significantly. Preliminary examinations have shown that the present scheme of power system planning and operations may face difficulty in the future. Especially, an issue of power system security will be a critical problem in the operation planning as well as in real-time operation. So far power system security has been maintained based on the N-1 security criterion, which has been refined through various basic studies on the security control scheme [1-3], relating optimal power flow method [4-11], and various techniques supporting the scheme [12-14]. These methods are deterministic and highly depend on accuracy of load forecast and prediction of system conditions. Therefore, new measures as well as effective methods [15-19] are studied based on the extension of deterministic approaches. However, uncertainties caused by RE will be beyond a level that existing methods can be adequately treated. In general, RE outputs sometimes behave very fast and the uncertainty in their behavior considerably increases as a function of the prediction time for future issues. On the other hand, the available capacities of controllable generations and their ramp-rates are very limited. In this relation, the authors have proposed a new concept of "Robust Power System Security" by extending the conventional N-1 security criterion [20-22].

Novel methodologies for dynamic economic load dispatch (DELD) have become necessary to guarantee secure operation in real-time scenarios. The ramping behavior of the system must be carefully maintained together with uncertainty. This particular concern is common to various widely-adopted power systems, where smart gird projects make use of all available controls including demand response. As the role of thermal power plants continues to increase, robust and reliable load dispatching methods are made necessary. Various techniques have been proposed so far concerned with DELD problem, classified into two approaches. The first approach performs static ELD repeatedly at each interval by taking into account the ramp rate constraints [23, 24]. The second approach

978-1-4799-0199-9/13/$31.00

determines GS by solving a single optimization problem and includes heuristic technique in dynamic programming [25], improved simulated annealing [26, 27], hybrid approach of Hopfield neural network and quadratic programming (QP) [28], variable scaling hybrid differential algorithm [29], re-dispatch algorithms using QP, linear programming and the Danzig Wolfe's decomposition technique [30], a multi-stage algorithm [31], and the interior point method [32]. As the expansion of the renewable energy generation continues, decreased number of controllable resources is necessary to be utilized utmost.

Feasibility and optimality are the improvement goals in [33] where non-monotonic load is taken into account. In the conventional approaches demand is assumed feasible for dispatch and generation schedule (GS) does not vary greatly. Important issue with conventional generation is that it might not respond adequately to sudden variations in renewable generation. Consequently forecast error such as high fluctuation and fast changes in the load might cause infeasibility for the dispatch. To cope with the forecast error, GS should be updated frequently, guarantying the dispatch feasibility with optimal reserve management (RM) within available computation limits. A fast reliable DELD method satisfying these requirements has been proposed by the authors in [34, 35]. Computing feasible operation region allows dealing with uncertainty to avoid infeasibility of GS. However, the network constraints such as overload are not implemented. Difficulty exists in treating network constraints since they become probabilistic variables when uncertainty cannot be neglected. Stochastic load flow (SLF) [36, 37] is a powerful tool for network analysis related to wind farms [38], network reliability [39], distribution network with PV and WT [40]. Those approaches effectively evaluate networks in a probabilistic manner, but are not useful for DELD problem. Thus, novel real-time DELD method is required to guarantee system security against increasing uncertainties in load and RE forecast.

In this paper, the conventional N-1 security criterion is extended to define a new criterion, Robust Power System Security based on the previous studies in [20-22]. The new criterion has the same concept as the conventional method except the treatment of uncertainties. Robust Static and Dynamic Security regions, RSS and RDS, are defined respectively for snapshot state and for dynamic state transition, as the regions of power system operation in which the system is secure regardless of existing uncertainties such as RE outputs. The concept of confident intervals is used to model uncertainties of important parameters. When the confident intervals of uncertain parameters are specified, RSS and RDS are identified. The concept has been introduced referring to the "robust stability" which implies the stability of a system under a pre-specified set of uncertainties.

Then, a new real-time DELD method is proposed to provide the solution in RSS and RDS guaranteeing secure operation while optimizing the outputs of controllable generators. Security constraints for transmission lines are only taken into account as security factor, while other factors are neglected such as transient stability and voltage stability. A DELD approach in [34] and GS update technique in [35] are extended to meet the condition for the new concept of the robust security. The proposed method computes 24 hour GS, where 1 hour update is performed every 5 minutes in real-time operation. New proposals of this paper includes the use of confidence intervals for load and RE forecasts, an algorithm for identifying robust regions for DELD, security constraints based on linear SLF, a new formulation of QP using all these techniques.

Another important issue discussed in this paper is the difficulties in the robust power system security concerned with transient stability (TS) problem [41]. Analysis is performed in an equivalent 3-machine system assuming the future circumstance in West Japan system. It is shown that, as REs are increased, the RSS as well as RDS regions shrink and finally disappear due to uncertainties. Since TS is critical factor among the security factors in the West Japan system, the results should be carefully investigated to develop countermeasures.

Definition of Robust Power System Security

Conventional N-1 Security Criterion

In this section, the conventional N-1 deterministic security criterion is represented by a set of equations in order to be extended to a new criterion. First, we express the power flow equations before and after contingencies as follows.

$$\left.\begin{aligned} &\boldsymbol{f}^n(\boldsymbol{x},\boldsymbol{u},\boldsymbol{p})=0 \\ &\boldsymbol{f}^n:\mathbb{R}^{\boldsymbol{B}+\boldsymbol{G}+\boldsymbol{L}}\to\mathbb{R}^{\boldsymbol{B}},\ \boldsymbol{u}_{min}\le\boldsymbol{u}\le\boldsymbol{u}_{max}, \\ &\boldsymbol{x}\in\mathbb{R}^{\boldsymbol{B}},\ \boldsymbol{u}\in\mathbb{R}^{\boldsymbol{G}},\ \boldsymbol{p}\in\mathbb{R}^{\boldsymbol{L}},\ n=0,1,\cdots,N \end{aligned}\right\} \quad (1)$$

Where, f is the power flow equation ($\boldsymbol{B}$ dimensions), x is state variable vector, u is control variable for output power of generation ($\boldsymbol{G}$ dimensions), p is uncontrollable fluctuation parameter such as load ($\boldsymbol{L}$ dimensions). Concerned with the power flow equation $\boldsymbol{f}^n$, n=0 represents pre-fault operation condition and n=1~N stand for the contingency conditions to define N-1 security criterion. In power system operation planning, while load $\boldsymbol{p}$ is predicted, generation output power u matching load $\boldsymbol{p}$ is determined. When pre-fault parameter ($\boldsymbol{u}$, $\boldsymbol{p}$) is given, $\boldsymbol{x}$

of equation (1) is determined for each condition n and we describe $x^0 \sim x^N$ for each condition, where x^0 indicate pre-fault condition and $x^1 \sim x^N$ denote fault conditions. We suppose that, once ($\boldsymbol{u}$, $\boldsymbol{p}$) is determined, it does not change before and after the fault. After all, the N-1 security criterion is satisfied with the following constraints for all $x^0 \sim x^N$ conditions.

(C1) Transmission line or transformer limit

$$g^{C1.n}(x^n, u, p) \le 0 \ , \ n = 0,1,\cdots,N \tag{2}$$

(C2) Voltage limit

$$g^{C2.n}(x^n, u, p) \le 0 \ , \ n = 0,1,\cdots,N \tag{3}$$

(C3) Voltage stability limit

$$g^{C3.n}(x^n, u, p) \le 0 \ , \ n = 0,1,\cdots,N \tag{4}$$

(C4) Transient stability limit

$$g^{C4.n}(x^n, u, p) \le 0 \ , \ n = 0,1,\cdots,N \tag{5}$$

(C5) Frequency deviation (power supply and demand control)

$$g^{C5.n}(x^n, u, p) \le 0 \ , \ n = 0,1,\cdots,N \tag{6}$$

Where, inequality above can be composed of all factors over vector functions. Equations (2) and (3) express the constraints for transmission and voltage limit, and can be solved by simple calculations. Equation (4) expresses the constraint for voltage stability implying to calculate maximum load point. Equation (5) expresses the constraint for transient stability. Equation (6) expresses the constraint for frequency deviation. By using mathematical expressions above, the objective of the operation planning is to determine control variable u of generation output power to satisfy equations (1)~(6) under given load condition p . In the following, we summarize the equations (2)~(6) as follows:

$$\left.\begin{aligned} & g^n(x^n, u, p) \le 0 \qquad n = 0,1,\cdots,N \\ & g^n = [g^{C1.n}, g^{C2.n}, g^{C3.n}, g^{C4.n}, g^{C5.n}] \end{aligned}\right\} \tag{7}$$

Where $u_{\min} \le u \le u_{\max}$, x^n is the solution of $f^n(x, u, p) = 0$

SS Region Satisfying N-1 Criterion

Satisfying N-1 security criterion for given load p is equivalent to determining control variable u inside the region where a set of constraints (1) and (7) holds for all contingencies. That is,

$$\left.\begin{aligned} & SS_u(p) = \{u \mid SS_{0,u}(p) \bigcap SS_{1,u}(p) \bigcap \cdots \bigcap SS_{N,u}(p)\} \\ & SS_{n,u}(p) = \{u \mid u_{\min} \le u \le u_{\max}, \ f^n = 0, \ g^n \le 0\} \\ & n = 0,1,\cdots,N \end{aligned}\right\} \tag{8}$$

We call the region "Static Security (SS) region" defined for a snapshot of power system operation at specific time. SS region is the region of generator outputs satisfying N-1 security criterion for specific parameter values of p. Power system operating point inside SS region is equivalent to that the system state is secure based on the N-1 security criterion.

Security Criterion Considering Uncertainties

Estimation of fluctuation parameter such as load forecast is very important for power system operation. Expressing $p(t)$ for such a fluctuation parameter vector at time t, we assume the following form of estimation formula.

$$p(t) = \hat{p}(t \mid t - \delta t) + \Delta(\delta t) \quad n = 0,1,...,N$$

$$\Pr\{\underline{\Delta}(\delta t) < \Delta(\delta t) < \overline{\Delta}(\delta t)\} = CL, \quad 0 \le CL \le 1 \tag{9}$$

Where, the first term in (9) is the forecast of $p(t)$ predicted at t-δt, and the second term is the forecast error, referred to as "uncertainty" in this paper. The uncertainty is characterized by the confidence interval, upper and lower bounds with confidence level CL. The uncertainty usually becomes larger as forecast time δt increases. In this paper we will take a standpoint that confident level is specified so that the upper and lower bounds of uncertainty are treated by deterministic approach. Confidence region of p is defined by the confidence intervals of their elements as follows.

$$R_P\{p \mid \hat{p} + \underline{\Delta} < p < \hat{p} + \overline{\Delta}\} \tag{10}$$

The expression permits uncertainty Δ around prediction $\hat{p}$ for selective value of confidence level, whose concept is given in Fig. 1. Practically, maximum forecast error in p

may be regarded as Δ. Power system planning and operation task is usually based on four stages, which are yearly system planning (reinforcement planning, expansion planning), electric power demand-supply planning from monthly to weekly, day ahead operation planning, and real-time operation.

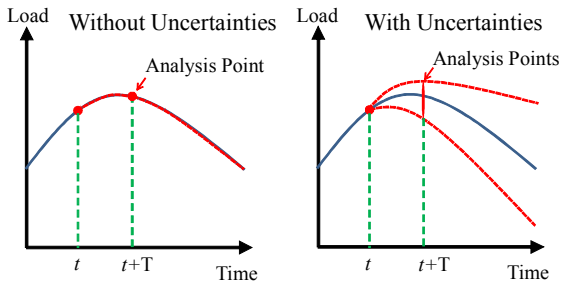

Fig.1. Confidence region for uncertain parameters.

For each stage, we examine power system security. In the conventional power system operations, p of load power is almost patterned and rather easily forecasted, where uncertainties are small. However, as RE is largely penetrated, the outputs may be fluctuated due to weather condition causing larger forecast error and then the power system planning and operation tasks should consider directly Δ of uncertainties. When the uncertainties exist in the confidence region of (10), the region of generator output power satisfying N-1 security criterion is reduced and is defined as the intersection of SS region with the parameter variations as follows.

$$RSS_u = \{u \mid u \in \bigcap_{p \in R_p} SS_u(p)\} \tag{11}$$

We define the region above Robust Static Security (RSS) region. RSS is the region of control variable u satisfying N-1 security criterion regardless of the existence of uncertainty.

Dynamic Feasible (DF) Region

Generators have dynamic operation constraints such as output power change rate limitation, or ramp-rate constraint due to thermal stress. Unit commitment and reactive power control problems are with such constraints. For example, control from $u(t_1)$ to $u(t_2)$ is constrained by a bound as a function of control duration δt. This kind of dynamic constraints may be represented as follows.

$$h(u(t_1), u(t_2), \delta t) \le 0 \tag{12}$$

Suppose that the state (x_1, u_1, p_1) at t_1 is given as starting point and that p_2 at t_2=t_1+δt is also given. Then, the next operation point (x_2, u_2, p_2) at t_2 will be determined satisfying power flow equation and (12). The region may be mathematically represented by:

$$DF_{u2}(u_1, p) = \{u_2 \mid h(u_1, u_2, \delta t, p_1, p_2) \le 0, f^0(x_2, u_2, p_2) = 0\} \tag{13}$$

We define this region as Dynamic Feasible (DF) region. DF region is defined as the region where generators can reach with maximum usage of power supply capacity from u_1 *of* generators output power at t_1 to u_1 at t_2 based on electric power demand forecast p_2. DF region does not necessarily take into account security constraints but takes into account the dynamic constraints and the power flow equations, implying the minimum constraints for the system operation such as demand and supply balance constraint. A sequential calculation method of DF is given in [20-22], which is discussed in the latter chapter in this paper, taking into account upper and lower limitation of generator output power, ramp-rate constraint and power demand and supply balance constraints based on load forecast. Next, we introduce uncertainties to the computation of DF region for consistency with RSS. Taking into account parameter confidence region based on equation (10), we define Robust Dynamic Feasible (RDF) region as follows.

$$RDF_{u2}(u_1) = \{u_2 \mid u_2 \in \bigcap_{p_1 \in R_{p1}, p_2 \in R_{p2}} DF(u_1, p)\} \tag{14}$$

Note that RDF is not related to security issues but defines possible operation region δt ahead reachable from u_0 under the specified uncertainty.

Dynamic Robust Security Region

Suppose that we draw up the operation planning considering uncertainties at several time points. From the viewpoint of continuity of the time sequence of the planning, we expand the concept of RS to dynamic approach. In the conventional power system operation planning, it used to be a common practice that only static analysis is performed to examine snapshot power flow without taking into account dynamic constraints. Direct extension of this approach is corresponding to the determination of RSS regions at different time points in advance before the dynamic transition examination. We assume that RSSs at t=t_1 and t=t_2 are determined in advance by the static snapshot analysis. Then, the set of u_1 at t_1 reachable to RSS at t_2 will be identified, which is represented by the region satisfying next equation.

$$RTA_{u1} = \{u_1 \mid (RDF_{u2}(u_1) \bigcap RSS_{u2}) \ne \phi\} \tag{15}$$

Thus we define the equation above as robust reachable region for Time-Ahead security (RTA). The region at t_1 going back from overlap region of RDF and RSS at t_2 is defined as RTA. In other words, RTA is the operation region not necessarily inside RSS at t_1 (not necessarily secure at t_1) but reachable to a secure point inside RSS at t_2.

After all, Robust Static Securities at t_1 and t_2 can be guaranteed only when u_1 exists within the overlap region of RSS and RTA, implying secure at t_1 and secure dynamic path for operation at t_2. In this paper, we define this overlap region as RDS region as follows.

$$RDS_{u1} = \{u_1 \mid u_1 \in RSS_{u1} \bigcap RTA_{u1}\} \quad (16)$$

The concept of the regions for robust security is shown in Fig. 2. This figure explains that every kind of regions are defined in the space for control vector u, generation output power at t_1 and t_2, and that for this duration the security is guaranteed only when we set up operation point u within RDS. In other words, RDS guarantees the conventional N-1 security in the sense that uncertain parameters must exist in their confidence region. The size of confidence region may vary depending on the accuracy of forecasting of parameters and on a specified confidence level. The more the uncertainties are increased, the larger is the confidence region and the smaller is RDS, implying the difficulty of secure operation.

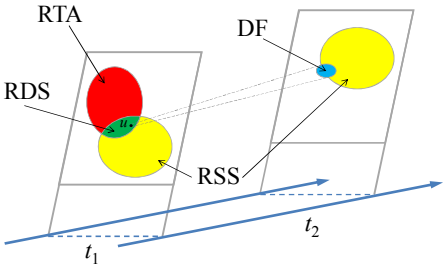

Fig.2. Concept of robust security regions.

Robust Security Region for DELD

In the following section, we consider real-time DELD problem, where the problem is more restricted in that the system is under operation on-line. We extend the DF region of (13) to a time sequence problem starting with a fixed operation point u_0 at present, which restricts subsequent operation regions. Then, taking into account the condition for the on-line time-sequence circumstance, we define Time-sequence DF (TDF) region as follows.

$$TDF_u(t,p) = \{u(t) \mid u(\tau) \in DF_{u(\tau)}(u(\tau-1),p),\ \tau = 1..t, u(0) = u_0\} \quad (17)$$

Note that $TDF_u(t, p)$ is function of parameters $p(1),\ldots, p(t)$ in (13), and t=0 represents the present time with no uncertainty with fixed value of $u(0)$, the present operating point. The above region may be extended in the same way to Robust TDF (RTDF) dealing with uncertainties of the parameters to be forecasted as follows.

$$RTDF_u(t) = \{u(t) \mid u(t) \in \bigcap_{p_\tau \in R_{p\tau}, \tau = 1..t} TDF_u(t,p)\} \quad (18)$$

Where R_{pt} implies the confidence interval of $p(t)$. In the following section, we propose a method to determine RTDF and the operating point inside the robust security region in the intersection of RTDF and RSS as follows.

$$u(t) \in \{RTDF_u(t) \bigcap RSS_u(t)\} \quad (19)$$

The above region is more restricted than RDS and therefore is composed by $RDS_{u(t)}$ which guarantees the robust security. In the next section, although only overloading condition C1 is considered, a new approach for real-time DELD is proposed for treating uncertainties.

DELD Problem with Uncertainties

In this section, conventional DELD problem is investigated taking into account uncertainties. Transmission line or transformer limit in (2) is considered while the other security constraints are neglected. We assume that preliminary contingency analysis has been completed and then that the security limits of transmission line flow has been determined. Since treatment of uncertainty for the robust security is a main subject, we mainly focus on constraints in DELD problem rather than the objective in order to study the region of power system operation. Any objective function may be applied to the proposed method to be described.

The proposed method computes 24 hour GS, where 1 hour update is performed every 5 minutes in real-time operation. The time duration for the real-time GS is referred to as time horizon in this paper. The proposed method has the following characteristics:

(i) A novel DELD method using 1 hour forecast with confident intervals as functions of prediction time. The solution combines QP and liner SLF, where the probability of network constraint violation is a specified value.
(ii) Supply-demand balance in the entire time horizon is kept to the maximum (high feasibility of dispatch).
(iii) In case of a critical situation when the forecasted load cannot match the existing generator's capability, the method will detect the minimum amount of SDM in advance and handle it reliably for the considered time horizon.

DELD Problem

The conventional problem of DELD may be written as follows:

Minimize:

$$Cost = \sum_{t=1}^{T} \sum_{k=1}^{Ng} f_k(P_{Gkt}) \quad (20)$$

$$f_k(P_{Gkt}) = a_k P_{Gkt}^2 + b_k P_{Gkt} + c_k \quad (21)$$

Subject to:

i. Supply and demand balance constraint

$$\sum_{k=1}^{Ng} P_{Gkt} = P_{Dt} = \sum_{m=1}^{Nd} P_{Dmt} \tag{22}$$

ii. Generator output limit

$$\underline{P_{Gk}} \le P_{Gkt} \le \overline{P_{Gk}} \tag{23}$$

iii. Ramp-rate constraint

$$-\delta_k \le P_{Gk(t-1)} - P_{Gkt} \le \delta_k \tag{24}$$

iv. Security constraint for transmission line

$$LF_l \le F_l \le UF_l \tag{25}$$

v. Power flow equation (DC power flow method) See equations (40) in the following section.

Where P_{Gkt} : power output of k-th generating unit at time t, f_k : k-th generation cost, P_{Gkt} : output of generator k at time point t [MW], a_k, b_k, c_k : quadratic cost coefficients of k-th generator, P_{Dt} is total demand at time t [MW], P_{Dmt} : demand for load m at time t [MW], and δ_k : ramp-rate limit of generator k [MW/unit time]. Note that we use the index t=0 for the present moment point and t=T for the end point of the time horizon. The terms $\overline{P_{Gk}}$ and $\underline{P_{Gk}}$ are the upper and lower limit of generator output; UF_l and LF_l are the upper and lower bounds with respect to the transmission line l for security [MW].

Uncertainty Expression

In recent power system, uncertainty mainly exists in the power demand, including RE output and demand forecast. We assume that node injection powers for loads are probabilistic variables having the following characteristic:

$$E[P_{Dmt}] + \underline{\Delta}_{PDmt} < P_{Dmt} < E[P_{Dmt}] + \overline{\Delta}_{PDmt} \tag{26}$$

$$\Pr\{\underline{\Delta}_{PDmt} < \Delta_{PDmt} < \overline{\Delta}_{PDmt}\} = C, \quad 0 \le C \le 1 \tag{27}$$

Where E [*] is the expectation. When probabilistic density function for P_{Dmt} is available, the following confidence intervals may be computed from (27).

$$E[P_{Dt}] + \underline{\Delta}_{PDt} < P_{Dt} = \sum_{m=1}^{Nd} P_{Dmt} < E[P_{Dt}] + \overline{\Delta}_{PDt} \tag{28}$$

$$\Pr\{\underline{\Delta}_{PDt} < \Delta_{PDt} < \overline{\Delta}_{PDt}\} = C, \quad 0 \le C \le 1 \tag{29}$$

Algorithm for RTDF

In this section, an algorithm for RTDF is proposed by improving the method in [34, 35], where we have proposed a real-time DELD method in [35] based on the computation of TDF in [34]. The computation method of TDF will be explained first and then will be extended to RTDF as below.

TDF has been defined in (17) in a general form but is redefined for the set of constraint for the DELD problem first. TDF is defined as the region of generator output P_{Gkt} reachable from a specified operating point and satisfying all constraints (22)-(24) with load forecasts for t = 1,…,T. The upper and lower bounds of TDF for generator k at t are represented by ($\overline{\alpha}_{kt}$, $\underline{\alpha}_{kt}$). Then, TDF defined by (17) is expressed as follows.

$$TDF_{Pk}(t, P_D) = \{P_{kt} \mid \underline{\alpha}_{kt} \le P_{kt} \le \overline{\alpha}_{kt}\} \tag{30}$$

Note that P_D is parameter to define TDF, starting from P_{kt0} with predicted P_{Dt}. A TDF evaluation algorithm was proposed in [35], where the present operating point t=0 is used as a starting point in order to obtain reachable points successively in forward direction to t=T. The upper feasible operation limit $\overline{\alpha}_{kt}$ and lower feasible operation limit $\underline{\alpha}_{kt}$ are calculated for each committed generator k=1,…,N using the latest forecasted demand P_{Dt} , t=1,…,T.

The upper bound of TDF for each generating unit is decided by 3 variables below.

$$\overline{\alpha}_{kt} = \min\left\{\overline{P}_{kt}, \overline{M}_{kt}, \overline{\alpha}_{k(t-1)} + \overline{R}_{kt}\right\} \tag{31}$$

i. Unit k's maximum generation limit, $\overline{P}_{kt}$, the first term of (31). This is dictated by the physical limit and may include certain margin (reserves etc.).

ii. Unit k's generation limit considering the generating capability of other generating units and load, $\overline{M}_{kt}$, the second term of (31).This is the amount that unit k must generate in order to match the load when the other units' generation is fixed to their minimum output. It is described by the following equation.

$$\overline{M}_{kt} = P_{Dt} - \sum_{j=1, j\ne k}^{N_g} \underline{P}_j \tag{32}$$

iii. The upper bound restricted by ramp rate from the previous interval, $\overline{\alpha}_{k(t-1)} + \overline{R}_{kt}$, the third term of (31). The value of $\overline{R}_{kt}$ is the effective ramp rate limit decided by the minimum of δ_k and $\overline{N}_{kt}$.

$$\overline{R}_{kt} = \min\left(\delta_k, \overline{N}_{kt}\right) \tag{33}$$

where, δ_k is the physical ramp up limit of unit k. $\overline{N}_{kt}$ is the amount that unit k must ramp up when the other units ramp down at their ramp down limit in order to accommodate the load change as given below.

$$\overline{N}_{kt} = \left(P_{Dt} - P_{D(t-1)}\right) - \sum_{j=1, j\ne k}^{N_g} \left(-\delta_j\right) \tag{34}$$

With three variables defined above, the upper boundary of the feasible operation region of unit k at time t, can be calculated by using the following equation.

By setting $\overline{\alpha}_{k0} = P_{k0}$, the initial condition at the present output of generator k, the upper boundary of the feasible operation region for the whole time zone is sequentially calculated (t = 1 to $t = T$).
In the same way, the lower boundary of TDF is calculated using equations listed below.

$$\underline{M}_{kt} = P_{Dt} - \sum_{j=1, j\neq k}^{N_g} \overline{P}_j \tag{35}$$

$$\underline{N}_{kt} = \left(P_{Dt} - P_{D(t-1)}\right) - \sum_{j=1, j\neq k}^{N_g} \delta_j \tag{36}$$

$$\underline{R}_{kt} = \max\left(-\delta_k, \underline{N}_{kt}\right) \tag{37}$$

$$\underline{\alpha}_{kt} = \max\left\{\underline{P}_k, \underline{M}_{kt}, \underline{\alpha}_{k(t-1)} + \underline{R}_{kt}\right\} \tag{38}$$

Extension to RDS

TDF obtained in the previous section is represented as $TDF(t,\ P_{Dt})$ using the expression of (30), RTDF is computed by taking into account upper and lower tolerance $\overline{\Delta}_{PDt}$ and $\underline{\Delta}_{PDt}$ of the prediction error, that is,

$$RTDF(t) = \{TDF(t, \mathrm{E}[P_{Dt}] + \overline{\Delta}_{PDt}) \bigcap TDF(t, \mathrm{E}[P_{Dt}] + \underline{\Delta}_{PDt})\} \tag{39}$$

where " $\bigcap$ " implies the intersection. An extended algorithm is proposed as follows.

Detection of Possible Supply Demand Mismatch

Once the upper and lower limits are obtained, any output values P_{Gkt} inside the limits (4) are guaranteed as reachable in respect to the latest load forecast. In this algorithm, when $\overline{\alpha}_{k1} < \underline{\alpha}_{k1}$ is detected, TDF is nonexistent and the supply and demand mismatch (SDM) is able to be computed. In such case, SDM must be compensated by additional power provision or load reduction. After the management of SDM, recalculating TDF, optimization process is continued. Note that this case does not appear in normal operation if RM is properly performed in the preliminary operation planning stage.

Line flow Security Constraints to Define RSS

Since the prediction errors of load and RE result in line flow uncertainty, line flow constraints are treated in a probabilistic manner as presented on Fig. 3. The SLF method is applied in such a way that the probability of constraint violation is less than a specified value for each line, consistent with the specified confidence level in the entire analysis. Assuming the normal distribution for the prediction error characteristic, linear DC power flow calculation method is used to provide the most efficient computational time.

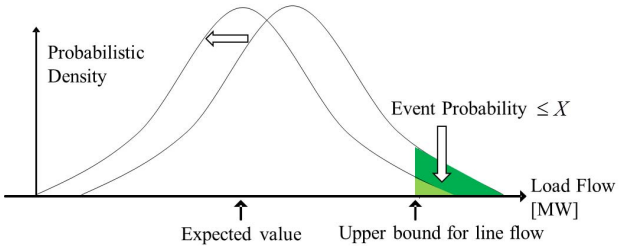

Fig. 3. Treatment of security limits by stochastic load flow.

Based on the DC power flow method, the following relationships hold.

$$\boldsymbol{S}_N \boldsymbol{\theta} = \boldsymbol{P} \tag{40}$$

$$\boldsymbol{F} = \boldsymbol{S}_C \boldsymbol{\theta} \tag{41}$$

Where, we introduce bold letters for vectors and matrixes. $\boldsymbol{\theta} \in \mathbb{R}^{Nn\times 1}$: voltage angle [rad], $\boldsymbol{P} \in \mathbb{R}^{Nn\times 1}$: real power injection [pu], $\boldsymbol{F} \in \mathbb{R}^{Nl\times 1}$: real power line flow, $\boldsymbol{S}_N \in \mathbb{R}^{Nn\times Nn}$: node susceptance matrix [pu/rad], $\boldsymbol{S}_C \in \mathbb{R}^{Nl\times Nn}$: line susceptance matrix. From (40) and (41), we obtain:

$$\boldsymbol{F} = \boldsymbol{S}_C \boldsymbol{S}_N^{-1} \boldsymbol{P} = \boldsymbol{S} \cdot \boldsymbol{P} \tag{42}$$

Node injection $\boldsymbol{P}$ is represented as

$$\boldsymbol{P} = \boldsymbol{P}_G - \boldsymbol{P}_D \tag{43}$$

Where $\boldsymbol{P}_D$ is a probabilistic variable consisting of loads and RE outputs (negative demands), while $\boldsymbol{P}_G$ corresponds to a variable of conventional generator outputs to be determined in the optimization process. Therefore, the mean value E [$\boldsymbol{P}$] of node injection power $\boldsymbol{P}$ is represented by the following expression:

$$E[\boldsymbol{P}] = \boldsymbol{P}_G - E[\boldsymbol{P}_D] \tag{44}$$

Then, the mean value vector and covariance matrix of line flow are represented as follows:

$$E[\boldsymbol{F}] = \boldsymbol{S}\left[\boldsymbol{P}_G - E[\boldsymbol{P}_D]\right] = \boldsymbol{S}\boldsymbol{P}_G - \boldsymbol{S} \cdot E[\boldsymbol{P}_D] = [u_i] \tag{45}$$

$$Cov[\boldsymbol{F}] = \boldsymbol{S} \cdot Cov[\boldsymbol{P}] \cdot \boldsymbol{S}^T = [\sigma_{ij}] \tag{46}$$

The probability density function for line flow l may be described using the elements from (45) and (46):

$$\xi_{F_l}(F_l) = \frac{1}{\sqrt{2\pi}\sigma_{ll}} \exp\left\{ -\frac{1}{2} \frac{(F_l - u_l)^2}{\sigma_{ll}^2} \right\} \quad (47)$$

In order to constrain the violation probability to a value less than X, threshold β is defined by the following equations.

$$X \geq 1 - \int_{\overline{F_l}}^{-\overline{F_l}} \xi_{F_l}(x) dx \quad (48)$$

$$\overline{F_l} - \beta \cdot \sigma_{ll} \geq \left| E[F_l] \right| \quad (49)$$

Note that X should be determined consistent with a required confidence level C in (9) and importance of constraints. Further substitution of (42) and (43) into (49), probabilistic power flow constraint is obtained.

$$LBF_l \leq \sum_{j=1}^{N_n} S_{lj} P_{Gj} \leq UBF_l \quad (50)$$

Where,

$$LBF_l = -\overline{F_l} + \beta \cdot \sigma_{ll} + D_l$$

$$UBF_l = \overline{F_l} - \beta \cdot \sigma_{ll} + D_l$$

$$D_l = \sum_{j=1}^{N_n} S_{lj} E[P_{Dj}]$$

$\overline{F_l}$: deterministic security limit for line l

Constraint (50) provides line flow limits, which must be consistent with the setting of (26)-(29). The method described above is to define RSS region for snapshot of time t, where the conditions vary depending on accuracy of prediction of P_{Dj} as well as σ_{ll} in (50). Therefore, constraint (50) is time variant and will be treated as a function of time in the next section.

DELD with Robust Security

In the previous section, we have proposed a method of determining RTDF region and of dealing with line flow constraints to define RSS region. In this section, an QP problem is formulated to provide a solution of DELD problem with uncertainty. The solution satisfies (19) guaranteeing the robust security. The DELD with uncertainties may be formulated as follows:

Minimize:

$$Cost = \sum_{t=1}^{T} \sum_{k=1}^{Ng} f_k(P_{Gkt}) \quad (51)$$

$$f_k(P_{Gkt}) = a_k P_{Gkt}^2 + b_k P_{Gkt} + c_k \quad (52)$$

Subject to:

i. Supply and demand balance constraint

$$\sum_{k=1}^{Ng} P_{Gkt} = \sum_{m=1}^{Nd} E[P_{Dmt}] \quad (53)$$

ii. Generator feasibility constraint

$$\underline{\alpha_{kt}} \leq P_{Gkt} \leq \overline{\alpha_{kt}} \quad (54)$$

iii. Ramp-rate constraint

$$-\delta_k \leq P_{Gk(t-1)} - P_{Gkt} \leq \delta_k \quad (55)$$

iv. Probabilistic network constraint

$$LBF_{lt} \leq F_{lt} = \sum_{j=1}^{N_n} S_{lj} P_{Gjt} \leq UBF_{lt} \quad (56)$$

Where $E[P_{Dmt}]$: expected demand for load m at time t [MW], S_{lj} : conversion matrix. UBF_{lt} and LBF_{lt} are the upper and lower bounds with respect to the transmission line l for security at time t [MW], which is the extension of (50) and is a new concept introduced in this paper. Robust security for future operating points up to T may be achieved at the present operating point at t=0 by the following steps 1-4 for t=1..T and step 5.

Step 1 Estimate P_{Dmt} and P_{Dt} for future time point t.
Step 2 Determine $\underline{\Delta}_{PDt}$ and $\overline{\Delta}_{PDt}$ in (29).
Step 3 Compute $\underline{\alpha_{kt}}$ and $\overline{\alpha_{kt}}$ based on (31), (38).
Step 4 Determine UBF_{lt} and LBF_{lt}.
Step 5 Solve QP problem (51)-(56).

Real-time Robust Control Scheme

Controller Configuration

Our goal is to develop a new type of smart grid controller that enforces robust security against uncertainties. Figure 4 shows the configuration of the control system being developed: there are three types of managers responsible

for day-ahead operation planning, minute-order real-time operation, and second-order real-time control. Based on the prediction of RE outputs, the system manages the existing generators, storage battery (BT) and demands in optimal manner. Detailed description of each of them is presented below.

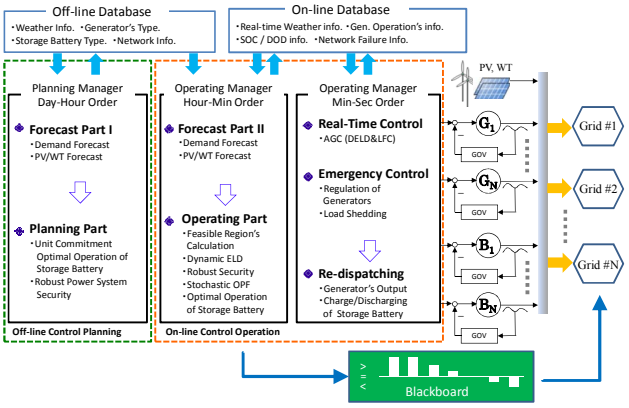

Fig. 4. Robust control manager.

Planning manager

This manager provides an updated schedule of the output pattern for the limited resources. The output is represented as a 24 hour GS which also comprises the battery operation schedule, where each unit of GS is 30 minutes. Existing techniques for the unit commitments have been fully utilized in the optimization process. Uncertainties related to the prediction and fluctuation of RE are handled particularly [42], and they will be discussed in a further publication.

Minute-Order Real-Time Manager

The manager releases real-time outputs for each generator based on the real time forecast values. The optimization is performed in two stages. In the first optimization, the 24 hour GS, which was planned in the previous day, is updated every 30 [min] from the present moment to fulfill a one hour schedule. Note that a one hour schedule is composed of 5-minute time units. In this stage, the starting and stopping time schedule is refined for the existing generators. The importance is related to significant impact on the prediction error. The next step utilizes only the starting and stopping time schedules and the battery operation. The rest of the optimization data is used only for reference. The second stage of optimization is the main topic of this paper. Scheme of the proposed method is given in Fig. 5, focusing on uncertainty managing process, which is explained in the next section. The procedure execution is performed every 5 minutes, which affirms substantial feasibility and robustness versus prediction error.

Entire Algorithm

(1) the 24 hour GS in the previous day
(2) 1 hour real-time GS with start/stop schedule
(3) 1 hour GS update in every control cycle (5 minutes) in which the following steps are performed.

Step A Perform load and RE forecasts (Steps 1 and 2). Estimate the current operating condition. Obtain a starting and stopping time schedule for generators and BT operation from 24 hour GS.

Step B Calculate RTDF (Step 3) and line flow limit (Step 4). Compute Supply-Demand Mismatch.

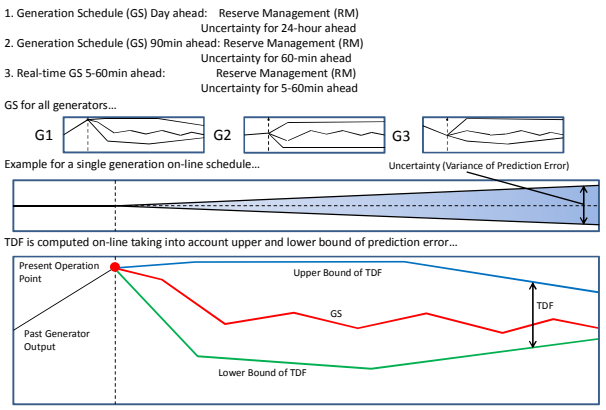

Fig. 5. Outline of a real-time GS and RM.

Step C If SDM appears, or if RSS region is nonexistence, arrange relevant reserve and update RTDF and/or line flow limit.

Step D Perform the optimization (Step 5) to provide real time GS, which will be sent to the generators as real-time control signal.

Examination of DELD

Simulation Conditions

The proposed method is demonstrated using an example system [42] in Fig. 6. Although the network is different, demand and supply data are prepared based on an ordinary Japanese smart grid project where the installed PV generation is about 15% of peak demand. It is composed of three diesel generators, two load areas with PV generations and a battery station. Detail data are given in Tables 1-3.

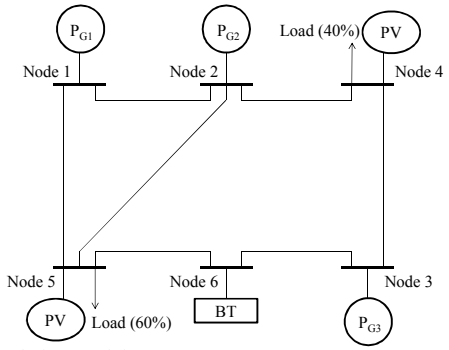

Fig. 6. Simulation model.

Typical weekday and weekend load patterns are used for the optimization process. Figure 7 shows the output of Day-ahead (DH) manager including the demand and PV output predictions, the total of generator outputs and BT operation given by 24 hour GS. In this stage of optimization, only the schedules for the starting and stopping time and for the battery operation are used.

Table 1 Specification of generators.

Unit k	$\underline{P_{Gk}}$ [kW]	$\overline{P_{Gk}}$ [kW]	δ_k [kW/min]	f_k
1	1000	2000	66.7	$0.0011P_1^2+16.416P_1+4320$
2	625	1250	41.7	$0.0021P_2^2+17.410P_2+3667.5$
3	1125	2250	75	$0.0002P_3^2+20.178P_3+3933.7$

Table 2 Start and stop times.

Demand pattern	Unit k	Start time	Stop time
Weekday	1	-	-
	2	14:20	17:20
	3	-	-
Weekend	1	-	-
	2	-	-
	3	-	-

Table 3 Line data.

Line No.	Reactance [ohm]	Line limits [kW]
1-2	0.06	-1200 ~ 1200
1-5	0.24	-650 ~ 650
2-4	0.03	-4600 ~ 4600
2-5	0.18	-900 ~ 900
3-4	0.24	-2000 ~ 2000
3-6	0.10	-2700 ~ 2700
6-5	0.06	-2700 ~ 2700

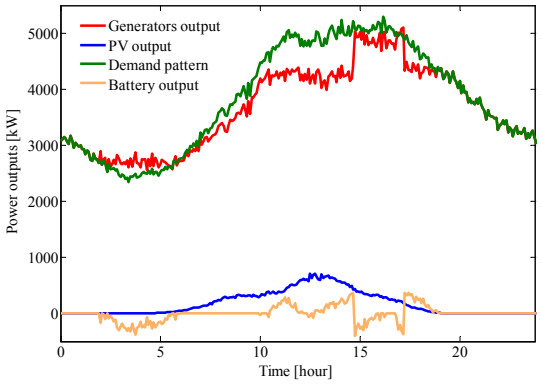

(a) Weekday

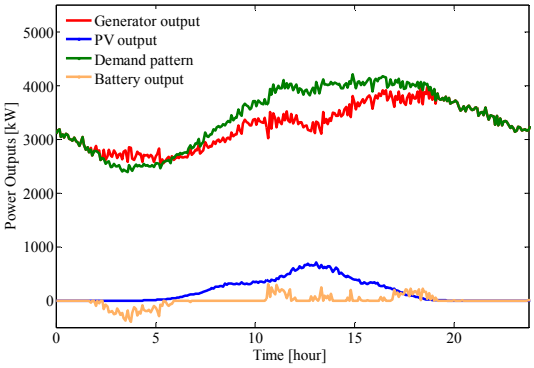

(b) Weekend

Fig. 7. Demand, PV and Battery operation patterns.

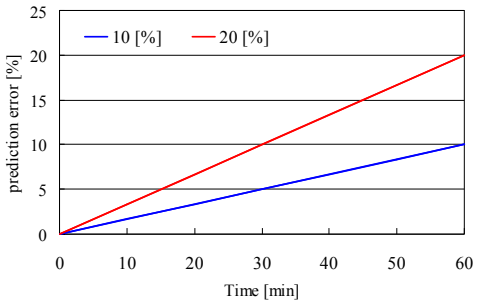

Fig. 8. The tolerances of prediction error

Although the rest of the data is just for reference, real-time demand prediction data are generated from the same data base and therefore Fig. 7 is informative.

$\overline{\Delta}_{PDt}$ and $\underline{\Delta}_{PDt}$ are set assuming that variances in the prediction errors increase linearly regarding time shown in Fig. 8. The upper and lower tolerances of prediction error are set as a linear function of time as follows:

$$\overline{\Delta}_{PDt} = \underline{\Delta}_{PDt} = P_{Dt} \times \frac{t}{T} \times \gamma \qquad (57)$$

Where $T = 60$ [min], t : prediction time ($t = 0$ for present operating point), γ is a parameter representing maximum prediction error, and [0%, 10%, 20%] will be examined. Allowable constraint violation for line flow is set to $X = 3\sigma = 0.26$[%] in this examination.

Results and discussions

Figure 9 shows GS for 1 hour ahead for weekday ($\gamma =$ 10%) at 13:45, including the upper and lower limits of TDF. As discussed before, the larger TDF, the larger system capability that copes with uncertainty is expected. It is observed that the feasibility of operation is guaranteed for 1 hour ahead in the GS. The most recent GS 5 minutes ahead is to be sent to each generating unit as a control signal. In this GS, P_{G2} will start-up at 14:20 to meet the increasing demand.

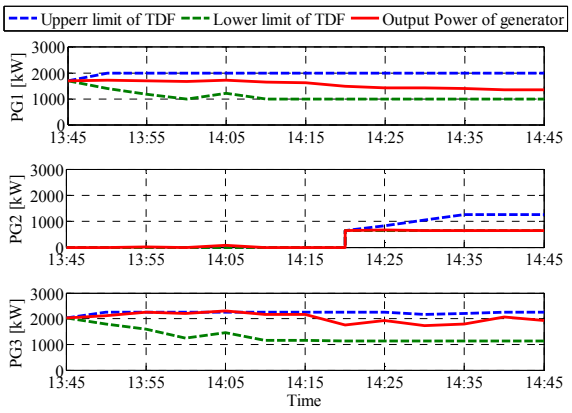

Fig. 9. Feasible region (RTDF) and GS during weekdays.

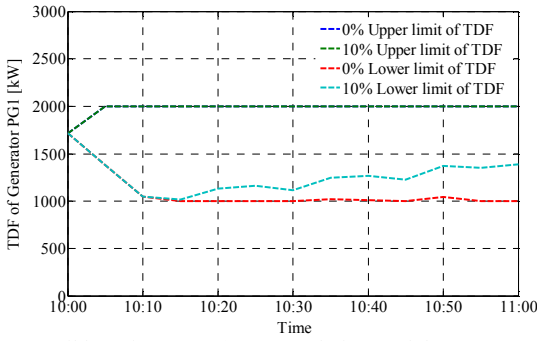

Fig. 10. Feasible region (RTDF) at 10:00 during weekdays.

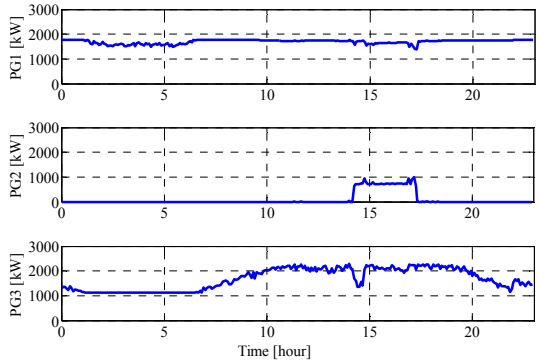

(a) During weekdays.

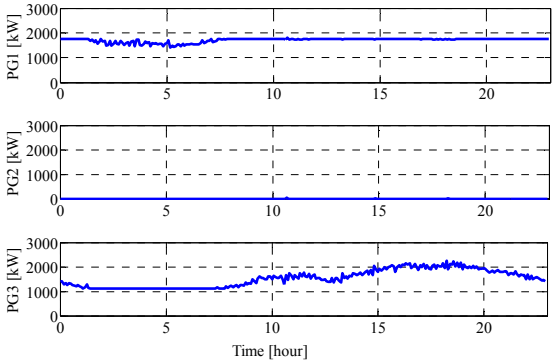

(b) Weekend

Fig. 11. The dispatch schedule.

Figure 10 compares TDFs in γ =0, 10%, showing the effect of different setting of prediction error limits. It is clearly seen that TDF shrinks as the prediction error tolerances increases.

Figure 11 shows the actual 1-day generation after the optimization process has been completed. Economic operation is attained, while coordinating uncertainty management. The network violation is successfully avoided by all means of the controllable resources, P_{G1}, P_{G2}, P_{G3} and BT.

Table 4 summarizes the fuel cost and CPU time for the total of 24 hour real-time computation for individual cases using Pentium P6200 2.13GHz. Stable computation is realized in all the cases.

Table 4 Fuel cost and CPU times.

Pattern	γ [%]	Fuel cost [yen]	CPU time [sec]
Weekday	0	1,759,200	21.2
	10	1,759,700	35.2
	20	1,760,400	48.9
Weekend	0	1,638,200	18.3
	10	1,638,400	18.3
	20	1,638,600	17.9

Concluding Remarks for DELD

Fluctuating levels of electricity production encountered from integrating large amounts of intermittent renewable energy into supply systems makes the demand-supply balance difficult to maintain. In this case, treatment of uncertainty is a critical issue by means of limited controllable resources.

Concept of Robust Security is proposed and its solution is demonstrated for DELD problem. Frequent evaluation of generation schedule takes important role in order to update Robust Security regions against prediction error and to establish a reliable and accurate operation response to the sudden changes in supply output. Although the computation time is a critical issue, the proposed method provides a solution for a grid operation where a large amount of RE resources is to be operated successfully.

Only the security limit for line flow is directly treated in the DELD problem, while effective approach is required to deal with the other stability factors. In the next section, the transient stability problem is investigated from the viewpoint of the robust security problem

Basic Examination of TS

Conditions for Simulation

A scope of this section is to provide clear examples of the problems arising in the operation planning tasks caused

by RE penetration. In order to demonstrate the concept of robust security, we hereby examine only transient stability (TS) for simplicity and neglect all other constraints such as transmission line thermal limits, voltage limits, voltage stability. We use simulation network of Fig.12 consisting of three areas, which is a dynamic equivalent obtained from the IEEJ West Japan 10-machine system. 3LG faults are considered at points A~C with fault clearing time, 70ms. There are several premises as follows.

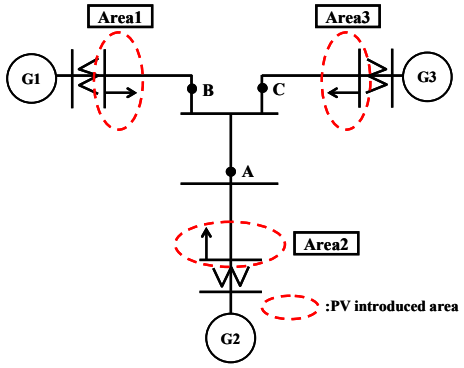

Fig. 12. Equivalent 3-machine model for West Japan system.

Table 5 PV Gen output power forecast.

	Area 1		Area 2		Area 3	
	Weather	PV1 [GW]	Weather	PV2 [GW]	Weather	PV3 [GW]
Case 1	Rain	0 ~ 2	Rain	0 ~ 1	Sunny	6
Case 2	Changeable	0 ~ 6	Changeable	0 ~ 6	Sunny	6

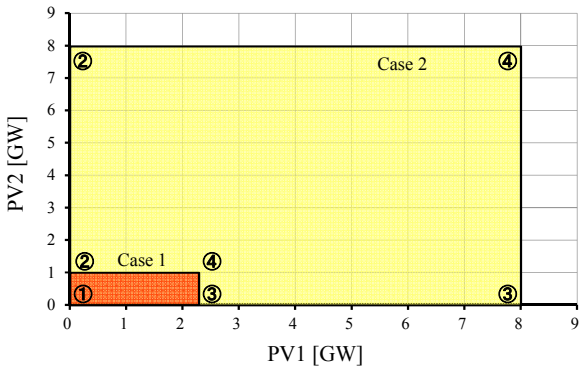

Fig.13. Setting of confidence region (PV Gen output power)

1. Photovoltaic generation (PV) is introduced at load terminals, up to 25% of total generation capacity and is simulated as negative load. Its electric power output is up to 70% of installed capacity.
2. Sufficient reactive power is supplied.
3. PV's output power fluctuation is compensated by generator G1~G3.

Outputs of PVs are treated as fluctuation parameter, which is uncertain a year before, but predictable one hour before. Thus, the size of uncertain may change depending on the purpose of analysis. In this examination, we set up two cases of PV's fluctuation with different sizes of uncertainties in Table 5 and in Fig. 13. Case 1 is with small uncertainty and case 2 with large uncertainty. In both cases, we assume that area 3 is sunny and PV generates 6,000MW. It is noted that the uncertain setting in this section may be controversial but provides important information concerned with inherent characteristic of TS problem against uncertainties. More realistic setting for future West Japan system will be presented in the next section.

Robust Static Security region (RSS)

RSS at *t* is analyzed by TS simulation. Case1 is studied through analysis at representative four points of PV outputs, expressed by circles 1~4 in Fig. 14. At each point of PV output, transient stability analysis is repeated by changing continuously the generator dispatch patterns to check stability. The set of analysis has been performed for faults A, B and C individually. The results are shown in Fig.15, where the individual regions within dotted lines indicate SS regions for different PV outputs at circles 1~4 in Fig.13. At planning stage where PV outputs have large uncertainty, we need to decide the operation point within the region overlapping all these SS regions.

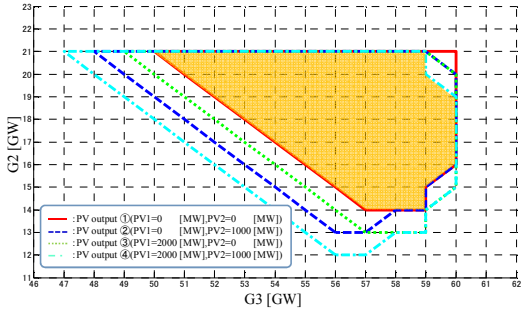

Fig.14. Robust static security region for case 1 (fault A)

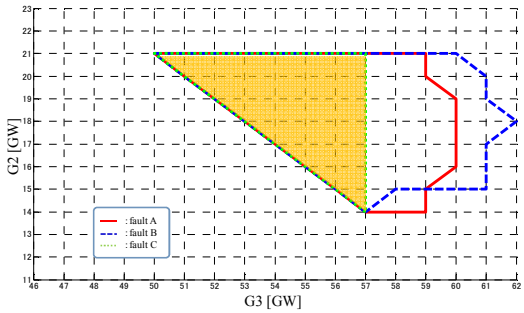

Fig.15. RSS region for case 1 (all faults A, B, C)

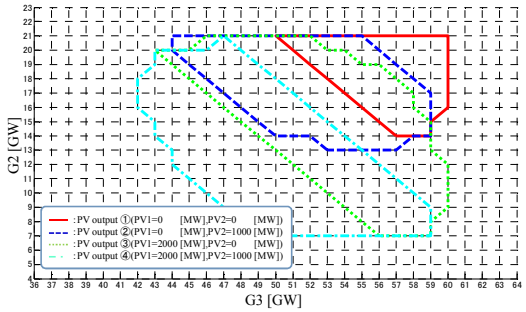

Fig.16. Nonexistence of RSS region for case 2 (all faults A, B, C)

Security analysis under large uncertainties (Case2)

Examination of RSS for fault point A is given in Fig.16. In this case, no overlap region is found, implying that RSS region disappears due to large uncertainty. The simulation result shows that, as uncertainties are becoming larger, RSS tends to shrink so that it may be difficult to keep operation point within RSS.

Robust Dynamic Security region (RDS)

Power system security analyses at t_1 and t_2 are performed to discuss dynamic transition and reachability through operating points using network in Fig. 12. Based on RSS at t_1 and t_2 obtained by transient stability analysis, we examine Robust Dynamic Security region (RDS). Suppose that load curve is given in Fig.17(a) and PV output powers at t_1 and t_2 are predicted as parameter fluctuation regions in Fig.17(b). Although unrealistic, no uncertainties are assumed in Area 3 where the output power of PV is constantly 6,000MW for simplicity. Based on the assumption, RSS is calculated at t_1 and t_2 in Fig. 18. In this examination, we set several point within RSS(t_2) in Fig.18 as the starting points of analysis and then calculate DF region backward from the starting points. RTA(t_1) is obtained as the sum set of the reachable points from the starting points.

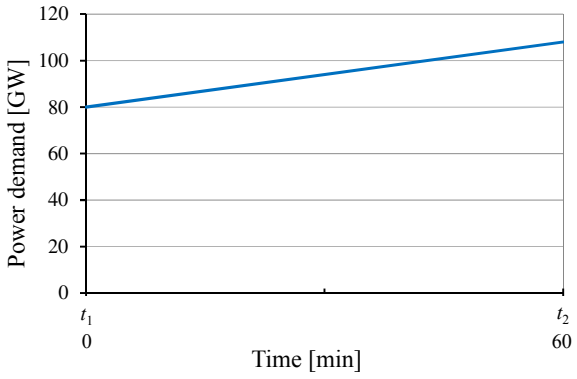

(a) Power demand increasing scenario from t_1 to t_2.

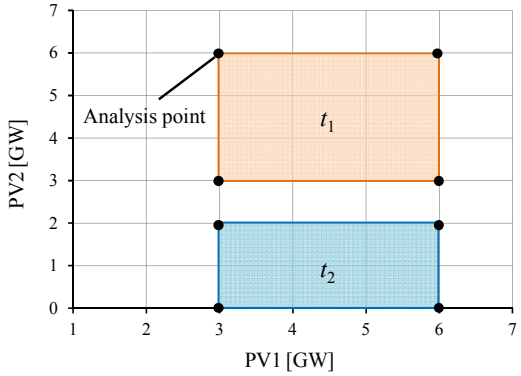

(b) Power output of PV generations at t_1, t_2.

Fig.17. Power demand and PV's output patterns.

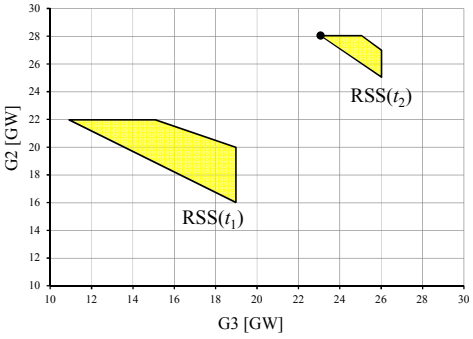

Fig.18. Transition of RSS.

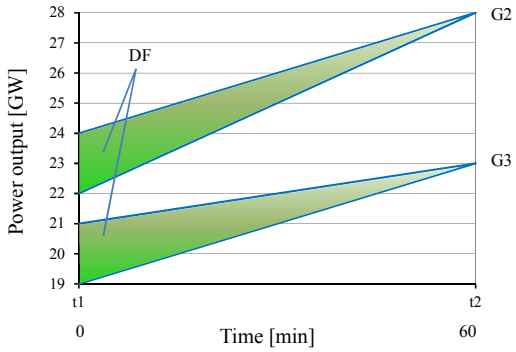

Fig.19. Backward dynamic feasible regions.

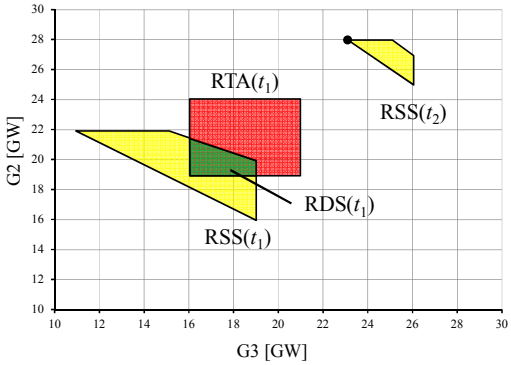

Fig.20. Robust dynamic security region (RDS).

An example of DF region at t_2 is given in Fig. 19, which is a set of the reachable points from SS at $t1$ in Fig. 18. By repeating this calculation, RTA is obtained in Fig. 20 as the region at t_1 reachable to RSS(t_2) within the dynamic capability of electric power supply facilities. Finally, we obtain RDS(t_1) as the intersection of RSS(t_1) and RTA.

An important observation is that, even though RSS is enough preserved in the static sense, only small RDS exists in this case. This implies that the operation planning taking account of dynamic transition of system states is a difficult task since the region of security itself shrinks with rapid change in loads, and furthermore, the shrink of the region is accelerated in the presence of uncertainty.

TS Examination for West Japan system

In this section, future conditions of the robust security of West Japan power system from present up to 2030 are analyzed from the point of view of transient stability. Other constraints such as thermal limits for transmission line, voltage limits and voltage stability are neglected. Static and dynamic characteristics of PV generations are studied based on the statistical analysis method in [43] applied to the weather data for West Japan, which is given in the Appendix. Then, using the PV generation characteristic data, the robust security analysis will be performed to compute RDS to investigate future conditions. The RDS will be used as a quantitative index for the N-1 security. Note that the examinations of this section are completely independent of those of previous section in the setting of parameters.

Model System for Simulation

The maximum load demand in 2010 for 60Hz power system in western part of Japan was 93GW and the maximum load demand in 2030 will be 108GW [41]. Since the original 60Hz power system is nearly 1,000 km in length from east to west and typical fish-bone type, it is rather easy to reduce the original system to a small equivalent system. We used the simulation model with three generators shown in Fig.12. Spinning reserve is secured 8% above the maximum load. Power supply capacities and maximum load demands at each area are shown in Table 6. The load demands at t_1=10 [min] and t_2=20 [min] are set up in Table 7 after preliminary examinations. In this time duration, the load following capability is quite important to be examined and is done by three generators. The ramp rate for each generator is set at 3%/min.

Table 6 Power supply capacities and peak load in each area in 2030.

[GW]	G1, Area1	G2, Aera2	G3, Area3	Total
Upper limit	20.5	21.5	74.0	116
Lower limit	6.5	6.5	22.5	35.5
Max. Load	19.5	20.0	68.5	108

Table 7 Load demands at t_1 and t_2 in 2030.

Time	t_0 (present)	t_1 (10 min. later)	t_2 (20 min. later)
Load [GW]	108.0	107.5	107.0

Conditions for daily load curve and PV

It is assumed that the daily load curves from the present up to 2030 are similar to each other where the yearly peak load will appear around 14 o'clock. All PVs are equipped with fault ride-through (FRT) function. That is, even in case of fault, all PVs keep operation without disconnecting from the power system. The characteristic of PV output fluctuation including treatment of the smoothing effect is given in the Appendix.

RDS as the benchmark for the N-1 security

The area of RDS will be used as a quantitative index for the N-1 security. First, 24 hour RDS is calculated from daily load curves in Fig. 21 using typical data for specific months, and the minimum value of RDS in each month is selected, given in Table 8, where low PV generation occurs in 2010. The minimum value of RDS is considered as the minimum level of the N-1 security. The result seems reasonable since the minimum RDS appears when yearly peak load is recorded. In this analysis, RDS is calculated for two cases with spinning reserves of 3% and 8%.

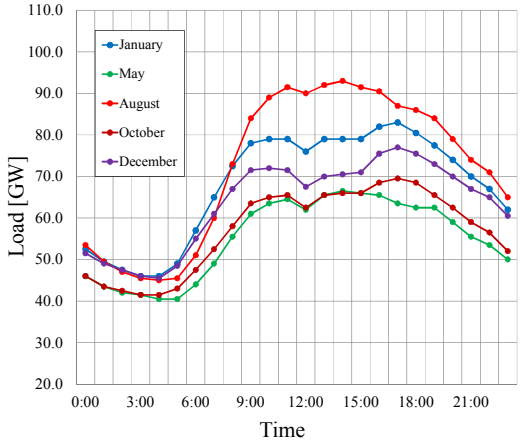

Fig.21. Typical daily load demand curves.

Table 8 RDS values.

	Jan.	May	Aug.	Oct.	Dec.
Peak Load (time)	83.0 (17:00)	66.5 (14:00)	93.0 (14:00)	69.5 (17:00)	77.0 (17:00)
RDS (3%) RDS (8%)	(a)53.1 (b)67.9	(a)109 (b)119	(a)4.5 (b)27.3	(a)100 (b)112	(a)74.4 (b)90.0

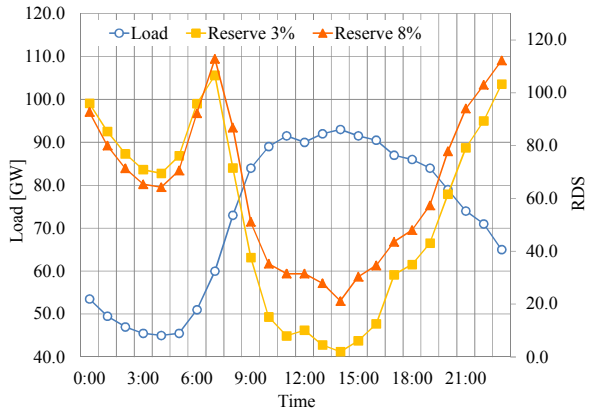

Fig.22. RDS and daily load demand curve for present power system.

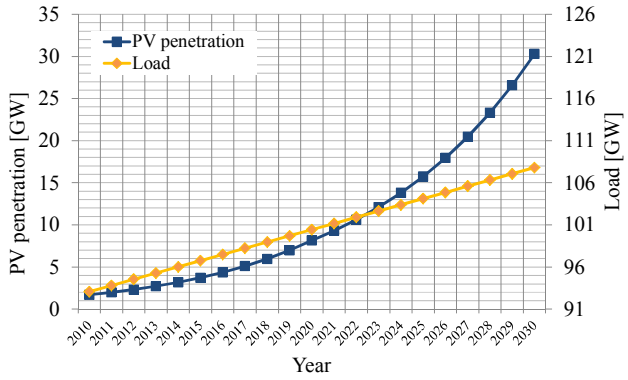

Fig.23. Scenarios of PV installation and load demand.

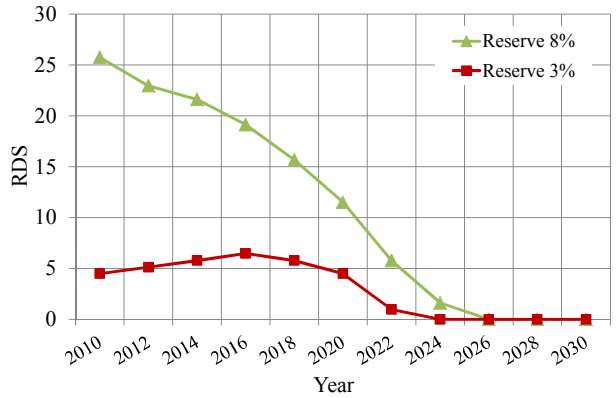

Fig.24. RDS at yearly maximum load demand.

Since the minimum RDS, most severe situation, appears in August (as shown in Table 8), the detailed data are shown on Fig. 22, where 24 hour RDS curves are given for August. It is observed that the values of RDS are 4.5 for 3% and 27.3 for 8%, which are used as the benchmarks for the security in 2010.

Future security with increased penetration of PV

Fig. 23 shows expected PV generation up to 2030, which correspond to target policy of the Japanese government. RDS of each year is calculated in a similar manner, given in Fig. 24.

Note that the starting points of RDS are the benchmark values mentioned before. According to the result, it can be stated that it is difficult to maintain the N-1 security level especially after 2020's.

Conclusion

A new concept of "Robust Power System Security" is proposed based on the modeling of uncertainties as well as the definitions of static and dynamic security regions, RSS and RDS. The forecast of loads and PV outputs must be properly modeled since their uncertainty cannot be eliminated. Over estimation will cause additional cost, while under estimation will result in system instability. Novel real-time DELD method is proposed, guaranteeing the power system operation in RDS regions.

The proposed method is useful for a limited size of power system but is questionable for a bulk power system at present since the frequent update of GS requires very fast computations, and most controllable power stations must be under the centralized control with severe output adjustment. The proposed method itself is robust and allows SDM, where no freedom of operating point exist and all the generators must produce specified outputs individually. Such a case contradicts the market based power system operation, implying that the increase in RE requires less market transactions and more integrated control to avoid system collapse.

Transient stability analysis assuming the future circumstance in Japan has shown that, as the REs are increased, the RSS as well as RDS regions shrink and will finally disappear due to the uncertainties. Although more detailed analysis is necessary, an effective countermeasure needs to be developed.

Furthermore, quantitative analysis is highly required to evaluate how much the security level is degenerated as functions of uncertainty. Since the security criterion actually determines the limit of power transfer, increase in uncertainty considerably affects the cost of power system operation. Analysis is important to describe the relationship among the security criteria, size of uncertainty and the cost of power system operation. The

actual cost of RE should be more exactly evaluated in this respect.

References

[1] T. E. Dy Liacco, “System security: the computer’s role,” IEEE Spectrum, pp.43-50, Jun. 1978.

[2] B. Stott and E. Hobson, ”Power System Security Control Calculations using Linear Programming, Part 1&2,” IEEE Trans. Power App. Syst. Vol. PAS-97, No.5, pp.1713-1731, Sep./Oct. 1978.

[3] M. H. Banakar and F. D. Galiana, “Power System Security Corridors Concept and Computation,” IEEE Trans. Power App. Syst., Vol. PAS-100, No.11, pp.4524-4532, Nov. 1981.

[4] B. Stott and J. L. Marinho, “Linear Programming for Power-System Network Security Applications, “ IEEE Trans. Power App. Syst., Vol. PAS-98, No.3, pp,837-848, May./Jun. 1979.

[5] J. L. Carpentier and G. Cotto, “Modern Concepts for Security Control in Electric Power System,” No. R-102-01, Proc. of CIGRE-IFAC Symp. on Control Applications to Power System Security, Florence, Italy, Sept. 1983.

[6] R. C. Burchett and H. H. Happ, “Large Scale Security Dispatching: An Exact Model,” IEEE Trans. Power App. Syst., Vol. PAS-102, No. 9, pp.2995-2999, Sept. 1983.

[7] B. Stott, O. Alsac, and A. J. Monticelli, “Security Analysis and Optimization,” Proceedings of the IEEE, Vol. 75, No. 12, pp.1623-1644, Dec. 1987.

[8] A. Monticelli, M. V. F. Pereira, and S. Granville, “Security-constrained Optimal Power Flow with Post-contingency Corrective Rescheduling,” IEEE Trans. Power Syst., Vol. PWRS-2, No. 1, pp.175-180, Feb. 1987.

[9] Y. Yuan, J. Kubokawa, and H. Sasaki, “A Solution of Optimal Power Flow With Multicontingency Transient Stability Constraints,” IEEE Trans. Power Syst., Vol. 18, No. 3, pp.1094-1102, Aug. 2003.

[10] M. M. Bhaskar, M. Srinivas, and M. Sydulu, “Security Constraint Optimal Power Flow (SCOPF) - A Comprehensive Survey,” International Journal of Computer Applications, Vol. 11, No.6, Dec. 2010.

[11] G. Hug-Glanzmann and G. Andersson, “N-1 Security in Optimal Power Flow Control Applied to Limited Areas,” IET Gener., Transm. Distrib., Vol. 3, No. 2, pp.206-215, Feb. 2009.

[12] G. D. Irisarri and A. M. Sasson, ”An Automatic Contingency Selection Method for On-line Security Analysis,” IEEE Trans. Power App. Syst., Vol. PAS-100, No.4, pp,1838-1844, Apr. 1981.

[13] K. Nara, K. Tanaka, H. Kodama, R. R. Shoults, M. S. Chen, P. V. Olinda, and D. Bertagnolli, “On-Line Contingency Selection Algorithm for Voltage Security Analysis,” IEEE Trans. Power App. Syst., Vol. PAS-104, No.4, pp. 847-856, Apr. 1985.

[14] N. Yorino, E. E. El-Araby, H. Sasaki, and S. Harada, ”A New Formulation for FACTS Allocation for Security Enhancement against Voltage Collapse,” IEEE Trans. on Power Syst., Vol.18, No. 1, pp. 3-10, Feb. 2003.

[15] H. Sun, D. C. Yu, and Y. Xie, “Flexible Steady-state Security Region of Power System with Uncertain Load Demand and Soft Security Limits,” Proc. of IEEE PES Summer Meeting, Vol. 4, pp.2008-2013, Jul. 2000.

[16] M. Ni, J. D. McCalley, V. Vittal, and T. Tayyib, “Online Risk-Based Security Assessment,” IEEE Trans. on Power Syst., Vol. 18, No. 1, pp. 258-265, Feb. 2003.

[17] E. A. Al-Ammar and M. A. El-Kady, “Application of Operating Security Regions in Power Systems,” Proc. of IEEE Transm. Distrib. Conf. Expo., pp.1-6, Apr. 2010.

[18] F. Bouffard, F. D. Galiana, and A. J. Conejo, “Market-Clearing With Stochastic Security - Part I & Part II” IEEE Trans. Power Syst., Vol. 20, No. 4, pp. 1818-1835, Nov. 2005.

[19] M. Power, “Stochastic power system operation,” Research Repository UCD, http://hdl.handle.net/10197/3208, 2010.

[20] N. Yorino, Y. Zoka, Y. Sasaki, K. Maruyama, N. Hiromitsu, Y. Onishi, and A. Sudo, “Static and Dynamic Feasible Operation Regions for Maintaining Security in Future Power System“ Proc. of IEEJ Annual Meeting, No.6-006, pp.11-12, Mar. 2009 (in Japanese).

[21] Y. Okumoto, N. Yorino, Y. Zoka, Y. Sasaki, T. Yamanaka, and T. Akiyoshi, “An Application of Robust Power System Security to Power System Operation for High-Penetration of PV,” Proc. of IEEE PES Innovative Smart Grid Technologies Conference (ISGT2012Europe) , No. 2012ISGTEU-016, Oct. 2012.

[22] N. Yorino, Y. Sasaki, S. Fujita, Y. Okumoto, and Y. Zoka, “Issues for Power System Operation for Future Renewable Energy Penetration: Robust Power System Security,” Electrical Engineering in Japan, Vol. 182, No. 1, pp. 30-38, Jan. 2013. Translated from IEEJ Trans. on Power and Energy, Vol. 131, No.8, pp.670-676, Aug. 2011.

[23] D. W. Ross and S. Kim, “Dynamic Economic Dispatch of Generation,” IEEE Trans. on Power App. Syst., Vol.PAS-99, No. 6, pp. 2060-2068, Nov. 1980.

[24] T. Li and M. Shahidehpour, “Dynamic Ramping in Unit Commitment,” IEEE Trans. on Power Syst., Vol. 22, No. 3, pp. 1379-1381, Aug. 2007.

[25] W. G. Wood, “Spinning Reserve Constrained Static and Dynamic Economic Dispatch,” IEEE Trans. on Power App. Syst., Vol. PAS-101, No. 2, pp. 381-388, Feb. 1982.

[26] D. N. Simopoulos, S. D. Kavatza, and C. D. Vournas, “Unit Commitment by An Enhanced Simulated Annealing Algorithm,” IEEE Trans. on Power Syst., Vol. 21, No. 1, pp. 68-76, Feb. 2006.

[27] C. L. Chen, “Simulated Annealing-based Optimal Wind-thermal Coordination Scheduling,” IET Gener. Transm. Distrib., Vol. 1, No. 3, pp. 447-455, May. 2007.

[28] A. Y. Abdelaziz, M. Z. Kamh, S. F. Mekhamer, and M. A. L. Badr, “A Hybrid HNN-QP Approach for Dynamic Economic Dispatch Problem,” Electric Power Systems Research, Vol. 78, No. 10, pp. 1784-1788, Oct. 2008.

[29] F. N. Lee, L. Lemonidis, and K. C. Liu, “Price-based Ramp-rate Model for Dynamic Dispatch and Unit Commitment,” IEEE Trans. on Power Syst., Vol. 9, No. 3, pp. 1233-1242, Aug. 1994.

[30] J. P. Chiou, “A Variable Scaling Hybrid Differential Evolution for Solving Large-scale Power Dispatch Problem,” IET Gener. Transm. Distrib., Vol. 3, No. 2, pp. 154-163, Feb. 2009.

[31] C. B. Somuah and N. Khunaizi, “Application of Linear Programming Redispatch Technique to Dynamic Generation Allocation,” IEEE Trans. on Power Syst., Vol. 5, No. 1, pp. 20-26, Feb. 1990.

[32] G. Irisarri, L. M. Kimball, K. A. Clements, A. Bagchi, and P. W. Davis, “Economic Dispatch with Network and Ramping Constrained via Interior Point Methods,” IEEE Trans. on Power Syst, Vol. 13, No. 1, pp. 236-242, Feb. 1998.

[33] X. S. Han, H. B. Gooi, and D. S. Kirschen, “Dynamic Economic Dispatch: Feasible and Optimal Solutions,” IEEE Trans. on Power Syst., Vol. 16, No. 1, pp. 22-28, Feb. 2001.

[34] H. M. Hafiz, N. Yorino, Y. Sasaki, and Y. Zoka, “Feasible Operation Region for Dynamic Economic Dispatch and Reserve Monitoring,” European Trans. on Electrical Power, Vol.22, No. 7, pp.924-936, Oct. 2012.

[35] N. Yorino, H. M. Hafiz, Y. Sasaki, and Y. Zoka, “High-speed Real-time Dynamic Economic Load Dispatch,” IEEE Trans. on Power Syst., Vol.27, No. 2, pp. 621-630, May. 2012.

[36] Borkowsk, B, “Probabilistic Load Flow,” IEEE Trans. on Power App. Syst., Vol. PAS-93, No. 3, pp.752-759, May. 1974.

[37] J. F. Dopazo, O. A. Klitin, and A. M. Sasson, “Stochastic Load Flows,” IEEE Trans. on Power App. Syst., Vol. 94, No. 2, pp. 299-309, Mar. 1975.

[38] O. A. Oke, D. W. P. Thomas, G.M. Asher, and L.R.A.X. de Menezes, “Probabilistic Load Flow for Distribution Systems with Wind Production using Unscented Transform Method,” Proc. of IEEE Innovative Smart Grid Technologies, pp.1-7, Jan. 2011.

[39] D.Dondera, R. Popa, and C. Velicescu, “The Multi-Area Systems Reliability Estimation Using Probabilistic Load Flow by Gramm-

Charlier Expansion," Proc .of EUROCON2007, pp.1470-1474, Sep. 2007.
[40] F. Rui-xiang, W. Su-nong, W. Yan, and H. Min-xiao, "The Analysis of Distribution System with Photovoltaic System Generation Based on Probabilistic Power Flow," Proc. of Power and Energy Engineering Conference Asia-Pacific (APPEEC), pp.1-5, Mar. 2011.
[41] Y. Okumoto, N. Yorino, Y. Sasaki, Y. Zoka, S. Fujita, T. Yamanaka, "Security Issues for Mega Penetration of PV in Future Electric Power System -A Case Study of Stability for Power Swing Oscillation using IEEJ WEST 10 Machines Model-," IEEJ Trans. on Power and Energy, Vol.132, No.2, pp. 171-180, Feb. 2012 (in Japanese)
[42] A. Tamaki, S. Yamada, N. Yorino, Y. Sasaki, and Y. Zoka, "Development of Power Supply and Demand Control Manager - Dynamic Economic Load Dispatch by means of Stochastic Load Flow-," IEEJ Joint Technical Meeting on Power Engineering and Power Systems Engineering, No. PE-12-084/PSE-12-100, pp.1-6, Aug. 2012 (in Japanese).
[43] A. Murata, H. Yamaguchi, and K. Otani, "A Method of Estimating the Output Fluctuation of Many Photovoltaic Power Generation Systems Dispersed in a Wide Area," Electrical Engineering in Japan, Vol.166, No.4, pp.9-19, Mar. 2009. Translated from IEEJ Trans. on Power and Energy, Vol. 127, No.5, pp.645-652, May. 2007.
[44] Japan Meteorological Business Support Center, "Ground weather survey data for 1 minute" Hiroshima Meteorological Observatory, 2010 (in Japanese)
[45] T. Oozeki, T. Takashima, K. Otani, Y. Hishikawa, G. Koshimizu, Y. Uchida, and K. Ogimoto, "Statistical Analysis of the Smoothing Effect for Photovoltaic Systems in a Large Area" IEEJ Trans. on Power and Energy, Vol.130, No.5, pp.491-500, May 2010 (in Japanese)

Appendix: Analysis of PV Output Power

PV output characteristics are analyzed by using the approach in [43] using the solar energy data provided by the Japan Meteorological Agency [44] for Hiroshima City. The solar energy data are directly converted to PV output powers assuming linear relationship between them. The smoothing effect is also taken into account to estimate PV output in the total area [45].

The fluctuation of PV output power is analyzed by an index of Fluctuation Rate (FR) [%] based on the approach in [43].

$$FR[\%] = \frac{\max\left[PV\ Output\right]_t^{t+T} - \min\left[PV\ Output\right]_t^{t+T}}{Installed\ Capacity\ of\ PV} \qquad (58)$$

Maximum and minimum values of solar energy are counted during the considered time interval T as shown in Fig. 25. The analysis is performed by sliding the time window from 8 o'clock to 16 o'clock to detect the maximum value of FR, which is defined as MFR [%]. MFR is measured as ±MFR, whose denominator is the installed capacity of PV. Analysis is performed for different time windows by using one month solar data for Aug. 2010 [43]. The result is shown in Fig. 26.

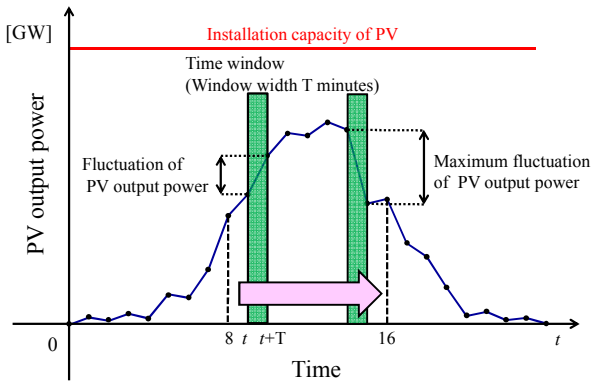

Fig. 25. Fluctuation rate of PV.

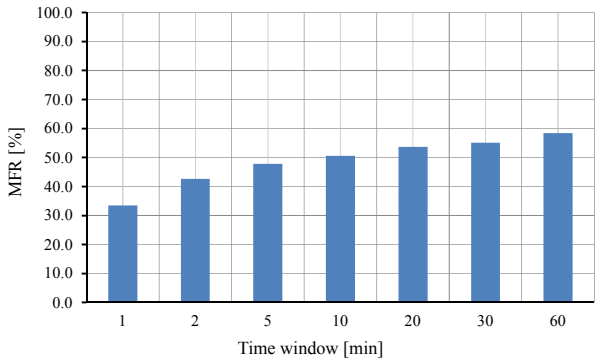

Fig. 26. *MFR* for different time window intervals

Since the solar data were observed at a specific location in the area [43], the smoothing effect is taken into account to estimate PV output in the total area. The analysis concerned with the smoothing effect has been established recently such as in [44]. In this paper, we adopted the smoothing effect coefficient 25% of the actual PV output where the area of 100 km in radius is considered [44]. The result is given in Table 9, which is used in the analysis taking into account the smoothing effect for the three independent areas.

Table 9 MFR with and without the smoothing effect.

	MFR (%)			
	1 min.	2 min.	10 min.	20 min.
MFR	33.5	42.6	50.6	53.7
MFR + smoothing effect	25.1	32.0	38.0	40.3